

Self-powered Photodetectors based on the Ga₂O₃/n-GaAs

V.M. Kalygina, O.S. Kisleleva, B.O. Kushnarev, Y.S. Petrova, A.V. Almaev,
V.L. Oleinik, A.V. Tsybalov*

Tomsk State University, Tomsk, Russia

*zoldmine@gmail.com

Abstract. The electrical and photoelectric characteristics of the Ga₂O₃/n-GaAs structures have been studied. A gallium oxide film was obtained by RF-magnetron sputtering on n-GaAs epitaxial layers with a concentration of $N_d = 9.5 \cdot 10^{14} \text{ cm}^{-3}$. The thickness of the oxide film was 120 nm. Measurements at a frequency of 106 Hz have shown that the capacitance-voltage and voltage-siemens dependences are described by curves characteristic of metal-insulator-semiconductor structures and exhibit low sensitivity to radiation with $\lambda = 254 \text{ nm}$. The samples exhibit the properties of a photodiode and are able to work offline when operating on a constant signal. The photoelectric characteristics of the detectors during continuous exposure to radiation with $\lambda = 254 \text{ nm}$ are determined by the high density of traps at the Ga₂O₃/GaAs interface and in the bulk of the oxide film.

Keywords: MIS structures, capacitance-voltage characteristics, volt-siemens characteristics, photocurrent, trap density.

1. Introduction

One of the promising directions in the development of shortwave radiation detectors are devices capable of operating in an autonomous mode. Self-powered photodetectors have a number of advantages over other devices based on wide-gap materials capable of detecting ultraviolet radiation. Such photodetectors have a simple design and, which is especially important, require direct integration with the technology of manufacturing metal-insulator-semiconductor (MIS) structures [1]. To date, a significant number of studies related to the study of the electrical and photoelectric characteristics of metal-Ga₂O₃-semiconductor structures have been described. Organic and inorganic materials were used as a semiconductor substrate [2–9]. The electrical and optical characteristics of such devices are determined by the choice of semiconductor, the technology and mode of obtaining the Ga₂O₃ film, and the technological methods used to process the oxide film after it has been deposited on the semiconductor substrate. This work presents the results of studies of the electrical and photoelectric characteristics of structures obtained by RF-magnetron sputtering of a gallium oxide film on n-GaAs epitaxial layers.

2. Experimental Details

The substrate was n-GaAs epitaxial layers with $N_d = 9.5 \cdot 10^{14} \text{ cm}^{-3}$. Epitaxial layers of electronic gallium arsenide 12 μm thick were grown on single-crystal GaAs (100) wafers. The thickness of the n+ buffer layer was 4.9 μm . After the deposition of the Ga₂O₃/n-GaAs oxide film, the structures were annealed in argon for 30 minutes at a temperature of 900 °C.

The phase composition of the film was studied using X-ray diffraction analysis (XRD) on a Lab-X XRD 6000 Shimadzu X-ray diffractometer. Studies of the atomic structure were carried out using an X-ray tube with a copper anode with a working wavelength of 1.54 nm.

Platinum contacts were deposited on the Ga₂O₃ surface and the rear side of the semiconductor substrate to measure the electrical characteristics of the samples. The contact to the semiconductor was deposited in the form of a continuous metal film, and the contact to gallium oxide was created by metal deposition through masks 1 mm in diameter. The area of the electrode to Ga₂O₃ (gate) was 1.04 cm².

Dark current-voltage characteristics (*I-V*) and *I-V* under UV radiation were studied at room temperature using a Keithley 2611V source-meter. A VL-6.C krypton-fluorine lamp with a 254 nm

filter was used as a source of UV radiation. The distance between the lamp and the sample was 1 cm, and the incident radiation intensity was 0.78 mW/cm^2 .

Capacitance-voltage (CVC) and voltage-siemens characteristics (VSC) of the obtained samples were measured at a frequency of 1 MHz. For this purpose, an E7-12 meter and a specially designed attachment were used, which made it possible to measure capacitance-voltage ($C-U$) and volt-Siemens ($G-U$) characteristics in one cycle in automatic mode and record data on a computer.

2. Results and Discussions

Fig.1 shows the results of analysis of a gallium oxide film obtained by RF-magnetron sputtering on a GaAs substrate after annealing in argon for 30 minutes at 900°C .

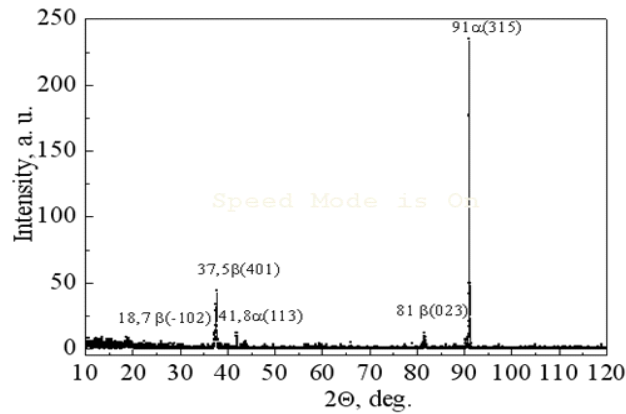


Fig.1. XRD results of a gallium oxide film after annealing in Ar at 900°C .

The Ga_2O_3 film contains β -phase crystallites oriented in the $[-102]$, $[401]$, and $[023]$ directions.

The $C-U$ and $G-U$ dependences of the samples (Fig.2) are described by curves characteristic of metal-insulator-semiconductor (MIS) structures. The thickness of the oxide film calculated by the flat capacitor formula from the dielectric capacitance in the enrichment mode ($C_d = 740 \text{ pF}$) is 124 nm.

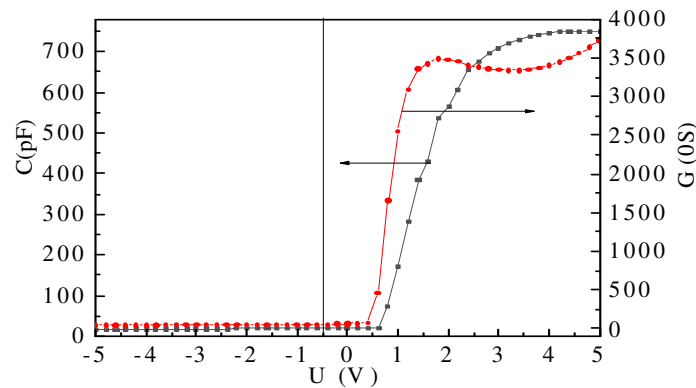


Fig.2. Volt-farad and volt-Siemens characteristics of the structure $\text{Ga}_2\text{O}_3/n\text{-GaAs}$.

The calculation of the charge carrier concentration in the semiconductor using the capacitance-voltage characteristic in the depletion mode showed that $N_d = 1.5 \cdot 10^{15} \text{ cm}^{-3}$, which, taking into account the experimental error, satisfactorily corresponds to the initial electron concentration in the epitaxial film. Thus, the deposition of a gallium oxide film by RF-magnetron sputtering does not

change the initial electron concentration in GaAs, in contrast to the production of a Ga_2O_3 film by electrochemical anodization [10].

Only a small increase in conductivity G is observed in the depletion mode (Fig.3) when UV radiation is turned on, the capacitive properties of the structure remain practically unchanged.

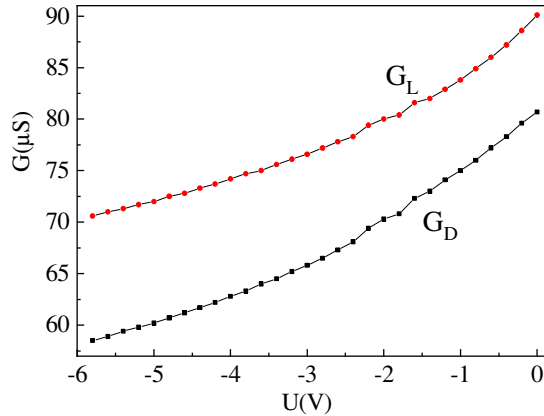


Fig.3. Volt-Siemens characteristics of the $\text{M}/\text{Ga}_2\text{O}_3/\text{n-GaAs}$ structure in the depletion mode: dark (G_D) and under UV irradiation with $\lambda = 254 \text{ nm}$ (G_L).

The dark current-voltage characteristics of the samples (I_D) are nonlinear and are determined by the sign and value of the gate potential (Fig.4). The rectification factor at voltages of $\pm 4 \text{ V}$ is 10^3 .

The forward current decreases and the reverse current increases under UV irradiation. The most noticeable effect of radiation with $\lambda = 254 \text{ nm}$ is observed at low positive and negative voltages on the sample, in the vicinity of $U \approx 0 \text{ V}$. Such structures have a voltaic effect and are usually characterized as self-powered photodiodes. For most of the samples studied in this work, the open-circuit voltage U_1 is $(0.40\text{--}0.43) \text{ V}$, and the short-circuit current I_{sc} is $(4\text{--}10) \cdot 10^{-7} \text{ A}$.

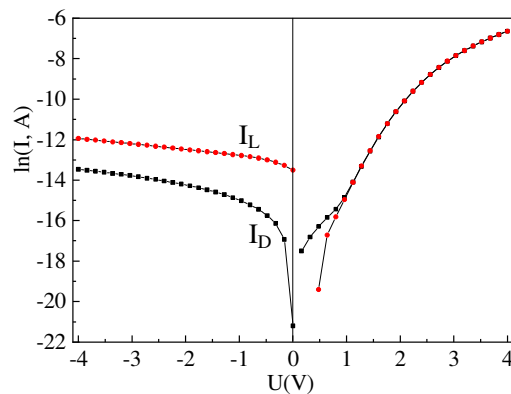


Fig.4. Current-voltage characteristics of the sample at positive and negative gate potentials: dark (I_D) and under UV irradiation with $\lambda = 254 \text{ nm}$ (I_L).

On a more detailed scale, the effect of UV radiation on the I - V characteristics of samples under continuous exposure (curves I_{L1} – I_{L5}) in Fig.5 is shown. The largest changes in the forward and reverse currents during UV radiation are observed during the first interrogation of the detector (I_{L1}) and decrease during subsequent measurements of the I - V during continuous exposure to UV irradiation (Fig.5, curves I_{L2} – I_{L5}).

Like many UV detectors based on gallium oxide films of the $M/\text{Ga}_2\text{O}_3/n\text{-GaAs}$ structure investigated in this work, they detect residual dark currents, indicated in Fig.5 as I_{D1} curves. The I_{D1} current was measured immediately after the UV irradiation was turned off.

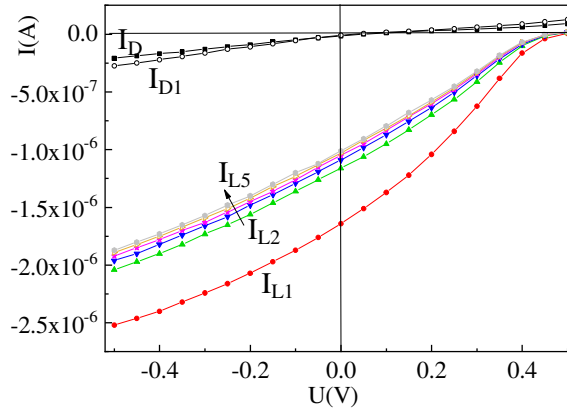


Fig.5. I - V of the sample at positive and negative gate potentials: dark (I_D , I_{D1}) and under UV irradiation with $\lambda = 254$ nm (I_{L1} - I_{L5}).

The studied $M/\text{Ga}_2\text{O}_3/n\text{-GaAs}$ structures reveal the properties of photodiodes operating in the voltaic regime. The reverse current increases by more than two orders of magnitude under UV irradiation with $\lambda = 254$ nm and voltage $U = -0.012$ V, which makes it possible to use such structures as detectors of UV radiation in the wavelength range of 200–280 nm. The influence of residual conductivity (persistent conductivity) on the temporal characteristics of the detectors is practically not observed at voltages close to zero. Fig.6 shows the change in the diode conductivity with time when the UV is turned on and off at a voltage of 0.005 V.

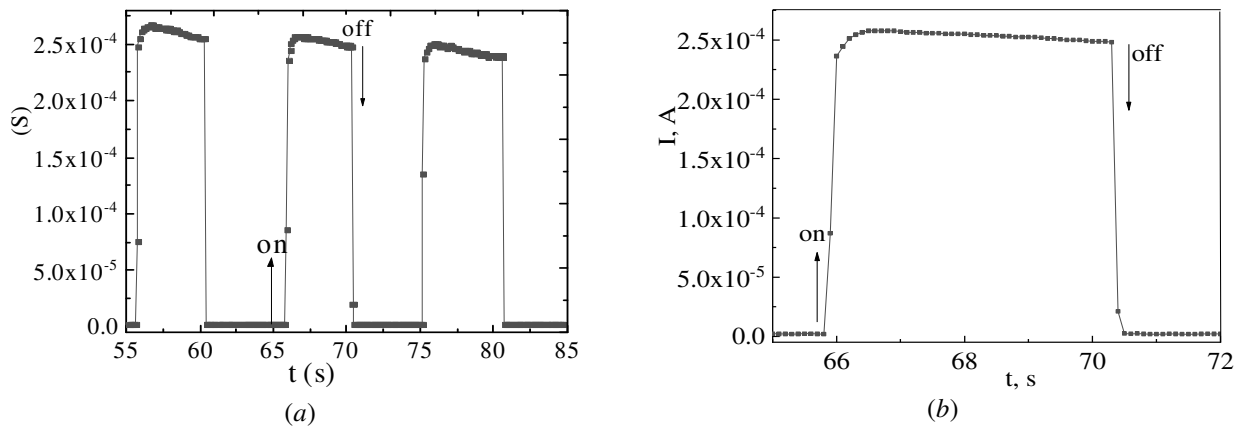


Fig.6. Time dependences of the change in the conductivity of the $M/\text{Ga}_2\text{O}_3/n\text{-GaAs}$ structure upon turning on and off the irradiation with $\lambda = 254$ nm (a); a single pulse on a more detailed time scale (b). $U = 0.005$ V.

The response time τ_r and the recovery time τ_f , determined by the level of 0.9 and 0.1, respectively, do not exceed 1–2 seconds; the recovery time τ_f at the level of 0.1 is – (1–2) seconds (Fig.6b), which is less than the time parameters of UV detectors based on barrier structures with interdigitated electrodes [11].

The decrease in photocurrent upon repeated action on structures during continuous exposure to UV radiation (Fig.5) is explained by the participation of trap centers in the formation of the response. The photocurrent is formed not only by the transition of electrons from the valence band to the conduction band, but also by the ejection of charge carriers from trap centers. The traps are

localized in the band gap of the oxide film and at the Ga₂O₃/GaAs interface [12–14]. Due to the large differences between the parameters of the Ga₂O₃ monoclinic lattice and the GaAs sphalerite lattice, it is assumed that there is a high density of surface states at the interface. As the traps are emptied, their contribution to the response decreases and the photocurrent stabilizes (Fig.5, curves I_{L2} – I_{L5}).

The density of N_t trapping centers at the Ga₂O₃/GaAs interface was estimated using the volt-farad and volt-siemens characteristics of MIS structures measured by the bridge method with capacitance (C) and conductivity (G) connected in parallel. The obtained values of C and G must be recalculated using formulas (1–3) in accordance with the equivalent circuit shown in Fig.7,

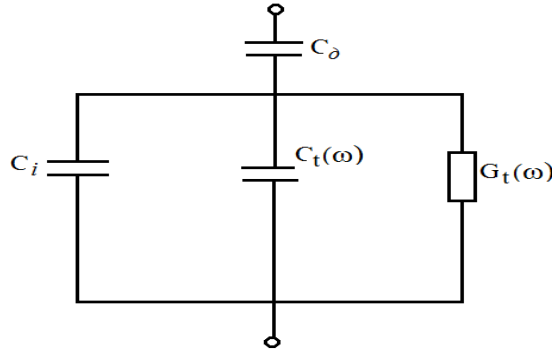


Fig.7. Equivalent circuit used to calculate the density of states at the Ga₂O₃/GaAs interface.

and obtain dependences $C_{sc}(\omega)$ and $G_t(\omega)/\omega$ [15]:

$$C_{sc}(\omega) = \frac{\omega^2 C_D^2 C - C_D (G^2 + \omega^2 C^2)}{G^2 + \omega^2 (C_D - C)^2}, \quad (1)$$

$$\frac{G_t(\omega)}{\omega} = \frac{\omega C_D^2 G}{G^2 + \omega^2 (C_D - C)^2}, \quad (2)$$

$$C_{sc}(\omega) = C_i + C_t(\omega). \quad (3)$$

In formulas (1–3) C_{sc} is the capacitance of the space charge region; C_D is the capacitance of the dielectric; C_t and G_t are, respectively, the differential capacitance and conductivity due to the recharging of surface states whose energy levels coincide with the Fermi level on the surface semiconductor F_s ; C_i is the capacitance of the inversion layer. To calculate the capacitance of the inversion layer, one can use the formula [15]

$$C_i = s \left(\frac{\epsilon \epsilon_0 e N_d}{2 |\phi_s|} \right)^{1/2}, \quad (4)$$

where s is the area of the electrode to the dielectric, ϵ is the permittivity of the semiconductor, ϵ_0 is the electric constant, ϕ_s is the surface potential. Experimentally, the capacitance C_i is found by determining the minimum value of the measured capacitance (C_{min}) on the CV characteristics at large negative biases on the MIS structure

$$\frac{1}{C_{min}} = \frac{1}{C_D} + \frac{1}{C_i}. \quad (5)$$

The voltage dependence of $G_t(\omega)/\omega$ is described by a curve with a maximum at the same voltage as the $G(U)$ curve in Fig.2. Using the data obtained in accordance with expression (2) and formula (6) [15]

$$\left(\frac{G_t}{\omega}\right)_{max} \approx 0.4e^2N_t(F_s), \quad (6)$$

the energy density of the traps was obtained $N_t = 3.2 \cdot 10^{13} \text{ eV}^{-1}\text{cm}^{-2}$. The found value of N_t characterizes the density of states only at the $\text{Ga}_2\text{O}_3/\text{GaAs}$ interface and, as noted above, is due to the mismatch between the lattice parameters of gallium oxide and gallium arsenide. The change in the photocurrent of $\text{Ga}_2\text{O}_3/n\text{-GaAs}$ structures during continuous exposure to radiation with $\lambda = 254 \text{ nm}$ is determined by traps not only at the interface, but also in the volume of the oxide film.

3. Conclusion

Gallium oxide film contains both alpha and beta phases. The electrical and photoelectric characteristics of $\text{Ga}_2\text{O}_3/\text{GaAs}$ structures obtained by RF-magnetron deposition of a gallium oxide film on $n\text{-GaAs}$ epitaxial layers with a concentration of $N_d = 9.5 \cdot 10^{14} \text{ cm}^{-3}$ are studied. The capacitance–voltage and voltage–siemens dependences of the samples are described by curves characteristic of metal–dielectric–semiconductor structures. The $\text{Ga}_2\text{O}_3/n\text{-GaAs}$ structures show a low sensitivity to radiation with $\lambda = 254 \text{ nm}$ measured at a frequency of 106 Hz. The samples exhibit the properties of a photodiode and are able to work offline working on a constant signal. The photoelectric characteristics of the detectors during continuous exposure to radiation with $\lambda = 254 \text{ nm}$ are determined by the high density of traps at the $\text{Ga}_2\text{O}_3/\text{GaAs}$ interface and in the bulk of the oxide film.

Acknowledgements

The work was supported by the Russian Science Foundation grant no. 20-79-10043.

4. References

- [1] Bae J., Park J., Jeon D., Kim J., *APL Mater*, **9**, 101108, 2021; doi: 10.1063/5.0067133
- [2] Sdoeung S., Sasaki K., Masuya S., Kawasaki K., Hirabayashi J., Kuramata A., Kasu M., *Appl. Phys. Lett.*, **118**, 172106, 2021; doi: 10.1063/5.0049761
- [3] Cui Y., Zhang S., Shi Q., Hao S., Bian A., Xie X., Liu Z., *Phys. Scr.*, **96**,125884, 2021; doi:10.1088/1402-4896/ac30a8
- [4] Li S., Yan Z., Liu Z., Chen J., Zhi Y., Guo D., Li P., Wu Z., Tang W., *J. Mater. Chem. C.*, **8**, 1292, 2020; doi: 10.1039/C9TC06011A
- [5] Yan Z., Li S., Yue J., Ji X., Liu Z., Yang Y., Li P., Wu Z., Guo Y., Tang W., *J. Mater. Chem. C.*, **9**, 5437, 2021; doi: 10.1039/D1TC00616A
- [6] Yan Z., Li S., Yue J., Liu Z., Ji X., Yang Y., Li P., Wu Z., Guo Y., Tang W., *J. Phys. Chem. Lett.*, **12**, 447, 2021; doi: 10.1021/acs.jpcclett.0c03382
- [7] You D., Xu C., Zhao J., Zhang W., Qin F., Chen J., Shi Z., *J. Mater. Chem. C.*, **7**, 3056, 2019; doi: 10.1039/C9TC00134D
- [8] H. Lin., Jiang A., Xing S., Li L., Cheng W., Li J., Miao W., Zhou X., Tian L., *Nanonamter.*, **12**, 910, 2022; doi: 10.3390/nano12060910
- [9] Tak B. R., Yang M.M., Lai Y.H., Chu Y.H., *Nature*, **10**, 16098, 2020; doi: 10.1038/s41598-020-73112-1
- [10] Kalygina V.M., Vishnikina V.V., Zarubin A.N., Petrova Yu.S., Skakunov M.S., Tolbanov O.P., Tyazhev A.V, Yaskevich T.M., *Izvestia Vysshikh Uchebnykh Zavedenii. Fizika*, **9**, 11, 2013; url: <https://www.elibrary.ru/item.asp?id=20397721>

- [11] Kalygina V.M., Tsymbalov A.V., Almaev A.V., Petrova Yu. S., *Semicond.*, **55**, 341, 2021; doi:10.1134/S1063782621030118
- [12] Armstrong A.M., Crawford M.H., Jayawardena A., Ahyi A., Dhar S., *J. Appl. Phys.*, **119**, 103102, 2016; doi: 10.1063/1.4943261
- [13] Frodason Y.K., Johansen K.M., Vines L., Varley J.B., *Appl. Phys.*, **127**, 075751, 2020; doi: 10.1063/1.5140742
- [14] Zhang Y.J., Shi J., Qi D., Chen L., Kelvin H.L., *APL Mater.*, **8**, 020906, 2020; doi: 10.1063/1.5142999
- [15] Gaman V.I., Ivanova N.N., Kalygina V.M., Sudakov E.B., *Izv. universities. Physics*, **11**, 99, 1992.